Article

Discovery Medicine 2025; 37(202): 2744–2757
https://doi.org/10.24976/Discov.Med.202537202.229

STAT6 Overexpression Attenuates Parkinson's Disease Pathology Through mTOR Activation

Xiaoqing Ma[1], Xiaoming Shi[2], Yu Li[3], Ling Cong[4], Hongbo Yao[5], Qi Lu[4], Yinan Tian[4,*]

[1]First Department of Neurology, The Third Affiliated Hospital of Qiqihar Medical University, 161000 Qiqihar, Heilongjiang, China
[2]South of the First Department of Bone, The First Hospital of Qiqihar, 161005 Qiqihar, Heilongjiang, China
[3]Health Center, Qiqihar Medical University, 161006 Qiqihar, Heilongjiang, China
[4]Second Department of Neurology, The Third Affiliated Hospital of Qiqihar Medical University, 161000 Qiqihar, Heilongjiang, China
[5]Department of Histology and Embryology, Basic Medical College, Qiqihar Medical University, 161006 Qiqihar, Heilongjiang, China
*Correspondence: tianyinan1234@163.com (Yinan Tian)
Submitted: 4 June 2025 Revised: 21 August 2025 Accepted: 12 September 2025 Published: 20 November 2025

Background: Parkinson's disease (PD) is a neurodegenerative disorder that affects motor and non-motor functions. However, the molecular mechanisms underlying PD remain unclear, and effective treatments are limited. Recent advances in single-cell RNA sequencing provide new insights into PD. Therefore, this study aims to explore cellular and molecular changes in PD using high-dimensional transcriptomic analysis.

Methods: This study analyzed single-cell RNA sequencing data (GSE157783) and gene expression data from the substantia nigra (GSE20292 and GSE20333). Dimensionality reduction and clustering identified 17 cell populations, and differential gene expression analysis identified signal transducer and activator of transcription 6 (STAT6) as a key regulator, which was further examined in PD model cells.

Results: Single-cell analysis revealed significant differences ($p < 0.05$) in specific cell populations between PD and control samples. STAT6 was identified as a key gene upregulated in both single-cell and tissue-level datasets. *In vitro* experiments showed that the overexpression of STAT6 in PD model cells reduced apoptosis and α-synuclein aggregation, while improving cell viability and migration ($p < 0.05$) by activating the mechanistic target of rapamycin (mTOR) signaling pathway. Conversely, STAT6 knockdown significantly increased apoptosis and aggregation of α-synuclein, and reduced cell viability and migration ($p < 0.05$). Additionally, the neuroprotective effect of STAT6-overexpression was significantly inhibited by the mTOR inhibitor, Rapamycin ($p < 0.05$).

Conclusion: This study highlights STAT6 as a key molecular regulator in PD, suggesting that targeting the STAT6-mTOR axis could be a promising therapeutic strategy in managing this disease. Future research should focus on further elucidating the role of STAT6 in the progression of PD and evaluating its therapeutic potential.

Keywords: Parkinson's disease; STAT6; single-cell transcriptomics; mTOR signaling; neuroinflammation

Introduction

Parkinson's disease (PD) is a progressive neurodegenerative condition marked by the deterioration of dopaminergic neurons within the substantia nigra. This neuronal degeneration results in motor impairments, such as tremors, muscle stiffness, and bradykinesia (slow movement), along with non-motor manifestations, including cognitive impairment and mood disorders, particularly depression [1]. Despite extensive research into its pathophysiology [1], the precise molecular mechanisms driving PD remain incompletely understood, and effective therapies targeting the underlying causes are limited. Recent advances in single-cell RNA sequencing have provided a powerful approach to examine the cellular heterogeneity within the brain and to unravel the complex molecular landscape involved in neurodegenerative diseases like PD [2].

Signal transducer and activator of transcription 6 (STAT6) has been implicated in various neuroinflammatory diseases [3] and is increasingly recognized for its role in the pathogenesis of PD through modulation of microglial activation and cytokine release. As a key transcription factor, STAT6 plays a crucial role in regulating immune responses, particularly by promoting T helper 2 (Th2) cell activation and modulating inflammation [4]. In the context of PD, emerging evidence has linked STAT6 with neuroinflammation, particularly the activation of M2 microglia, which are key mediators of neuroinflammatory responses [5]. Additionally, STAT6 influences several downstream pathways, including those that regulate apoptosis, cell survival, and tissue remodeling [6–8], all of which can significantly affect the progression of neurodegenerative diseases such as PD. Studies have indicated that reduced STAT6 expression exacerbates neuronal loss and impairs cell migration [8,9].

Hence, STAT6 is emerging as a crucial molecular regulator of inflammatory response and cellular dysfunction in PD, highlighting it as a promising therapeutic target to alleviate neuroinflammation and prevent neuronal degeneration in PD.

The mechanistic target of rapamycin (mTOR), a highly conserved serine/threonine kinase, is widely expressed across mammalian cell types, where it primarily regulates cell growth, proliferation, survival, metabolism, protein synthesis, and autophagy [10,11]. Recent studies have reported mTOR as a key modulator of neurodevelopmental processes, including neuronal maturation, maintenance, and phenotypic specialization, and have demonstrated its critical role in synaptic plasticity [12]. Recent evidence further indicates that dysregulation of mTOR signaling is implicated in PD pathogenesis, whereas its proper activation may exert neuroprotective effects [13,14].

Therefore, this study aims to elucidate cellular and molecular changes in PD using high-dimensional transcriptomic analysis. Our results show that STAT6 overexpression activates the mTOR signaling pathway, while inhibition of mTOR with Rapamycin significantly reduces cell apoptosis and viability in PD model cells. These findings suggest that the STAT6-mTOR axis may contribute to the pathophysiology of PD and highlight its potential as a therapeutic target.

Materials and Methods

Data Collection and Preprocessing

Three datasets were used in this study to investigate the role of STAT6 in Parkinson's disease (PD) through both single-cell transcriptomics and tissue-level gene expression analyses. The single-cell RNA sequencing dataset GSE157783 (https://www.ncbi.nlm.nih.gov/geo/query/acc.cgi?acc=GSE157783) was retrieved from the Gene Expression Omnibus (GEO) database, consisting of transcriptomic data of 41,435 cells derived from 6 control individuals and 5 PD patients. The tissue-level gene expression data were obtained from two GEO datasets: GSE20292 (https://www.ncbi.nlm.nih.gov/geo/query/acc.cgi?acc=GSE20292) and GSE20333 (https://www.ncbi.nlm.nih.gov/geo/query/acc.cgi?acc=GSE20333), both including substantia nigra samples from PD patients and normal controls. GSE20292 contains data from 15 controls and 11 PD patients, while GSE20333 includes 6 controls and 6 PD patients.

Single-Cell RNA Sequencing Data Analysis

Single-cell transcriptomic data analysis was performed using the Seurat package in R (version 4.0) for R, maintained by the Satija Lab, New York Genome Center, New York, NY, USA. The raw counts from GSE157783 were first processed to generate a Seurat object. Quality control filtering excluded cells with fewer than 200 detected genes or with mitochondrial gene expressions greater than 10%. The data were then normalized using the Seurat function "NormalizeData" with a log-transformation method. For dimensionality reduction, the data were scaled and subjected to principal component analysis (PCA), with the first 30 principal components selected for downstream analyses. Single-cell clustering was performed using the "FindClusters" function at a resolution of 0.5, and t-distributed stochastic neighbor embedding (t-SNE) was used for visualizing the clusters. Cell types were annotated using the SingleR package in R based on reference datasets for astrocytes, endothelial cells, and macrophages. Differentially expressed genes (DEGs) across all clusters were identified using the "FindMarkers" function in Seurat with an adjusted p-value threshold of <0.05.

Tissue-Level Gene Expression Analysis

Differential expression analysis of the gene expression data from GSE20292 and GSE20333 was conducted utilizing the DESeq2 package in R. Raw counts were normalized through the "DESeqDataSetFromMatrix" function, and differential expression between PD samples and controls was evaluated with the "DESeq" function. Genes with an adjusted p-value < 0.05 were identified as DEGs. Volcano plots were created with the "ggplot2" package to visualize significantly upregulated and downregulated genes. Overlapping DEGs between the two datasets were determined using Venn diagram analysis. Additionally, to investigate the biological processes, cellular components, and molecular functions related to these genes, Gene Ontology (GO) and Kyoto Encyclopedia of Genes and Genomes (KEGG) pathway enrichment analyses were performed using the "clusterProfiler" package in R.

Gene Expression Integration and STAT6 Analysis

The DEGs identified from both the single-cell and tissue-level analyses were integrated to unveil shared alterations in PD. STAT6 was identified as a predominantly upregulated gene in both datasets and was selected for further investigation. Furthermore, protein-protein interactions (PPIs) between STAT6 and other DEGs, focusing on those related to immune response and neuroinflammation, were assessed using the STRING database (https://string-db.org/).

Cell Culture and Transfection

Human neuroblastoma SH-SY5Y cells (American Type Culture Collection, ATCC, Manassas, VA, USA, #CRL-2266) were cultured in Dulbecco's modified Eagle's medium (DMEM, Gibco,11965126) supplemented with 10% fetal bovine serum (FBS, Solarbio, China, 11011-8611) and 1% penicillin-streptomycin at 37 °C in a humidified atmosphere with 5% CO_2. Cell lines were verified through short tandem repeat (STR) profiling, and cultures screened for mycoplasma contamination. To es-

tablish a PD cellular model, SH-SY5Y cells were treated with 1 mM 1-methyl-4-phenylpyridinium (MPP+, Sigma, D048) for 24 hours [15]. The effect of STAT6 overexpression and knockdown was investigated by transfecting cells with either a STAT6 expression vector (for overexpression) or siRNA targeting STAT6 (for knockdown). Transfection was conducted using Lipofectamine 2000 (Invitrogen, 11668500) following the manufacturer's instructions, and cells were collected 48 hours post-transfection for further analyses. The STAT6 gene was amplified using the following primers:

(Forward: 5′-ACCCTCGAGTCCGCCACCATGGCTCTGTGGGGTCTG-3′;

Reverse: 5′-CAGCTGGGATCGAATTCTGGGGTTGGCCCT-3′) and was then cloned into the pDsRed2-N1 vector (BD Biosciences Clontech) to generate an RFP-tagged overexpression construct. Cells transfected with the empty vector (EV) plasmids served as the control group for STAT6 overexpression experiments. Sequences of siRNAs are given in Table 1.

Apoptosis and Cell Viability Assays

Apoptosis was evaluated using Annexin V/propidium iodide (PI) staining. Following the manufacturer's instructions, cells (1×10^6/mL) were collected, rinsed, and labeled with Annexin V-FITC and PI (Beyotime, C1062) for 10 minutes in the dark. Apoptotic cells were quantified using a flow cytometer (BD Biosciences, NJ, USA, 95131), with subsequent data analysis performed through FlowJo software (Tree Star, Ashland, OR, USA).

Cell viability was determined using the MTT assay. Specifically, SH-SY5Y cells were cultured in 96-well plates and exposed to MPP+ (1mM) for 24 hours. Afterward, cells were incubated with MTT reagent (Sigma-Aldrich, St. Louis, MO, USA; #CT01) for 4 hours, and absorbance was recorded at 490 nm using a microplate reader (BioTek Instruments, Winooski, VT, USA, #Synergy H1). Cell viability was calculated by normalizing the absorbance of treated cells against that of untreated controls, after subtracting background signals from the blank wells.

Table 1. Sequences of siRNAs used in generating STAT6-knowdown construct.

siSTAT6-1	Forward: 5′-AGAAGAUCUUCAAUGACAACA-3′ Reverse: 5′-UUGUCAUUGAAGAUCUUCUGG-3′
siSTAT6-2	Forward: 5′-GGAGACCACUGGAGAGCUAGA-3′ Reverse: 5′-UAGCUCUCCAGUGGUCUCCUG-3′
siSTAT6-3	Forward: 5′-GGAAGCAGGAAGAACUCAAGU-3′ Reverse: 5′-UUGAGUUCUUCCUGCUUCCAG-3′
siNC	Forward: 5′-UUCUCCGAACGUGUCACGUTT-3′ Reverse: 5′-ACGUGACACGUUCGGAGAATT-3′

STAT6, signal transducer and activator of transcription 6; siSTAT6, small interfering RNA targeting STAT6; siNC, negative control siRNA.

Western Blot Analysis

Protein expression was assessed using Western blot analysis. Cells were harvested at 70–80% confluence, and cell lysates were prepared using RIPA buffer supplemented with protease inhibitors. Equivalent volumes of protein were resolved by SDS-PAGE and subsequently transferred onto PVDF membranes (MilliporeSigma, Burlington, MA, USA, IPVH00010). The membranes were blocked using 5% skim milk and then incubated with primary antibodies targeting STAT6 (1:1000, #9362), mTOR (1:1000, #2972), phosphorylated mTOR (p-mTOR, 1:1000, #5536), S6K (1:1000, #9202), phosphorylated S6K (p-S6K, 1:1000, #9234), 4EBP1 (1:1000, #9452), and phosphorylated 4EBP1 (p-4EBP1, 1:1000, #13443), all sourced from Cell Signaling Technology. Following incubation with horseradish peroxidase (HRP)-conjugated secondary antibodies (1:1000, Cell Signaling Technology, #7074, #7076), the protein bands were visualized using an ECL detection kit (Thermo Scientific, #34580). β-actin (1:1000, Cell Signaling Technology, #4967) served as the loading control. Protein bands were visualized using a commercial chemiluminescent substrate (Pierce Biotech Inc., Rockford, IL, USA, #32132) and captured using a ChemiDoc™ MP Imaging System (Bio-Rad, Hercules, CA, USA, ChemiDoc™ MP), with subsequent densitometric analysis performed using ImageJ (version 1.53) (National Institutes of Health, USA).

Immunofluorescence Staining

For immunofluorescence analysis, cells were first fixed with 4% paraformaldehyde (Beyotime Biotechnology, Shanghai, China, P0099-3L), permeabilized with 0.1% Triton X-100 (Beyotime Biotechnology, Shanghai, China, C1715), and subsequently blocked with a 5% bovine serum albumin. Samples then underwent overnight incubation at 4 °C with primary antibodies targeting α-synuclein (1:100, Proteintech, 10842-1-AP). The next day, samples were incubated with Alexa Fluor 594-conjugated secondary antibodies (1:50, Thermo Scientific, #A-11012). Nuclei were counterstained with DAPI (1:5000, Thermo Scientific, #D3571). Confocal images were acquired using an Olympus FV3000 confocal microscope (Olympus Corporation, Tokyo, Japan, FV3000) and quantified using the Image J software (Version 1.52a, NIH, Bethesda, MD, USA) by measuring mean fluorescence intensity across at least 3 fields per sample, background subtracted, from three independent experiments.

Wound Healing Assay

Cell migration was evaluated using a wound healing assay. SH-SY5Y cells were cultured at a density of 4×10^5 cells per well in 6-well plates and transfected with either a STAT6 overexpression vector or STAT6-targeting siRNA. After 24 hours, a sterile pipette tip (Thermo Fisher Scientific, Waltham, MA, USA, #712010) was used to create a

wound in the cell monolayer. Cells were then cultured in serum-free medium, and images were captured at 0 and 24 hours to measure the migration rate. The migration rate was assessed using the following formula: Migration rate (%) = $[(A_0 - A_{24})/A_0] \times 100$.

Real-Time PCR

Total RNA was isolated from cultured cells using RNAiso Plus (TaKaRa), and 2 µg of RNA was reverse-transcribed into cDNA using PrimeScript™ II reverse transcriptase (TaKaRa). Target transcript amplification was performed in qRT-PCR using SYBR Green (TaKaRa). For quantitative analysis, the expression levels of STAT6, iNOS, TNF-α, and IL-1β were normalized to β-actin and calculated using the $2^{-\Delta\Delta Ct}$ algorithm. The sequences of the qPCR primers used in this study are provided in Table 2.

Reactive Oxygen Species (ROS) Measurement

Intracellular ROS were quantified using the Cellular ROS Assay Kit (Abcam, #ab186029). Briefly, cell suspensions (200 µL, 1–1.5 $\times$ 10^5 cells) were incubated with 2 µL of the ROS detection reagent in 6-well plates at 37 °C for 30 minutes in the dark. Fluorescence intensity was subsequently determined at an excitation wavelength of 648 nm using a fluorescence microscope (LSM880, Zeiss, Germany). Mean fluorescence intensity was quantified using Image J software (Version 1.52a, NIH, Bethesda, MD) across at least 3 fields per sample, after background subtraction, from three independent experiments.

Statistical Analysis

Statistical analyses were conducted using GraphPad Prism (version 8.0, GraphPad Software, San Diego, CA, USA). Each experiment was independently repeated three times. Data normality was performed using the Shapiro-Wilk test. Results are expressed as the mean $\pm$ standard deviation (SD). Comparisons between two groups were performed using Student's *t*-tests, while multiple group comparisons were conducted using one-way ANOVA followed by Tukey's post-hoc test. For non-normally distributed data, comparison between two groups was performed using Mann-Whitney U test. Statistical significance was defined at a *p*-value of less than 0.05.

Table 2. Sequences of primers used in qRT-PCR.

STAT6	Forward: 5′-CTCGCTGGACAGAGCTACAG-3′ Reverse: 5′-GACTTGGAGGTTGCCTCGGA-3′
iNOS	Forward: 5′-GCACGGCAACACATTGAA-3′ Reverse: 5′-TGAGGTTCTGAAGGCCTAAATC-3′
TNF-α	Forward: 5′-AGGCGGTGCTTGTTCCTCA-3′ Reverse: 5′-AGGCGAGAAGATGATCTGACTGCC-3′
IL-1β	Forward: 5′-TGAAGCAGCTATGGCAACTG-3′ Reverse: 5′-CTGCCTTCCTGAAGCTCTTG-3′
β-actin	Forward: 5′-GACCCAGATCATGTTTGAGA-3′ Reverse: 5′-GCTTGCTGATCCACATCTGC-3′

iNOS, Inducible Nitric Oxide Synthase; TNF-α, Tumor Necrosis Factor-α; IL-1β, Interleukin-1β; qRT-PCR, Quantitative Reverse Transcription Polymerase Chain Reaction.

Results

Single-Cell Transcriptomic Profiling of Parkinson's Disease Using the GSE157783 Dataset

The GSE157783 dataset, comprising single-cell transcriptomic sequencing data of 41,435 cells derived from 6 control individuals and 5 Parkinson's disease (PD) patients, was retrieved from the GEO database. Single-cell analysis was conducted using the Seurat package in R to perform dimensionality reduction and clustering (Fig. 1A), resulting in the identification of 17 distinct cell populations. Cell types were annotated using the SingleR package in R, yielding an annotated dimensionality reduction cluster map (Fig. 1B). Annotation results revealed that clusters 0, 1, 2, 3, 4, 6, 7, 10, 11, 12, 13, 14, 15, and 16 corresponded to astrocytes, clusters 8 and 9 to endothelial cells, and cluster 5 to macrophages. Additionally, a heatmap of differentially expressed genes across all clusters was also generated (Fig. 1C). Based on sample characteristics, the cells were categorized into a control group (Group C) and a PD group (Group PD), and dimensionality-reduced clustering maps were generated for both groups (Fig. 2A). Analysis demonstrated that certain cell populations exhibited significant differences between the two conditions, particularly in 13 clusters where only data from normal samples were present, with no corresponding data from PD samples. Consequently, an individual-level percentage chart was generated, illustrating the proportion of each sample within each cell population (Fig. 2B). It was noted that although these 13 clusters originated from control samples, most of the data came from a single sample exhibiting deviation, leading to their exclusion from further analyses. Additionally, box plots were constructed, comparing the two groups based on the proportion of each cell population (Fig. 2C), revealing substantial differences in three specific clusters, 0, 2, and 5 ($p < 0.05$).

Differential Gene Expression Analysis of Substantia Nigra Tissue in PD Using the GSE20292 and GSE20333 Datasets

Substantia nigra matrices gene expression tissue associated with PD, specifically GSE20292 (15 normal controls and 11 PD cases) and GSE20333 (6 normal controls and 6 PD cases), were retrieved from the GEO database. Differential expression analysis was conducted using the "DESeq2" package in R, and volcano plots illustrating findings were generated with the "ggplot2" package (Fig. 3A for GSE20292, Fig. 3B for GSE20333). Intersection analysis across the two datasets yielded 29 co-upregulated genes

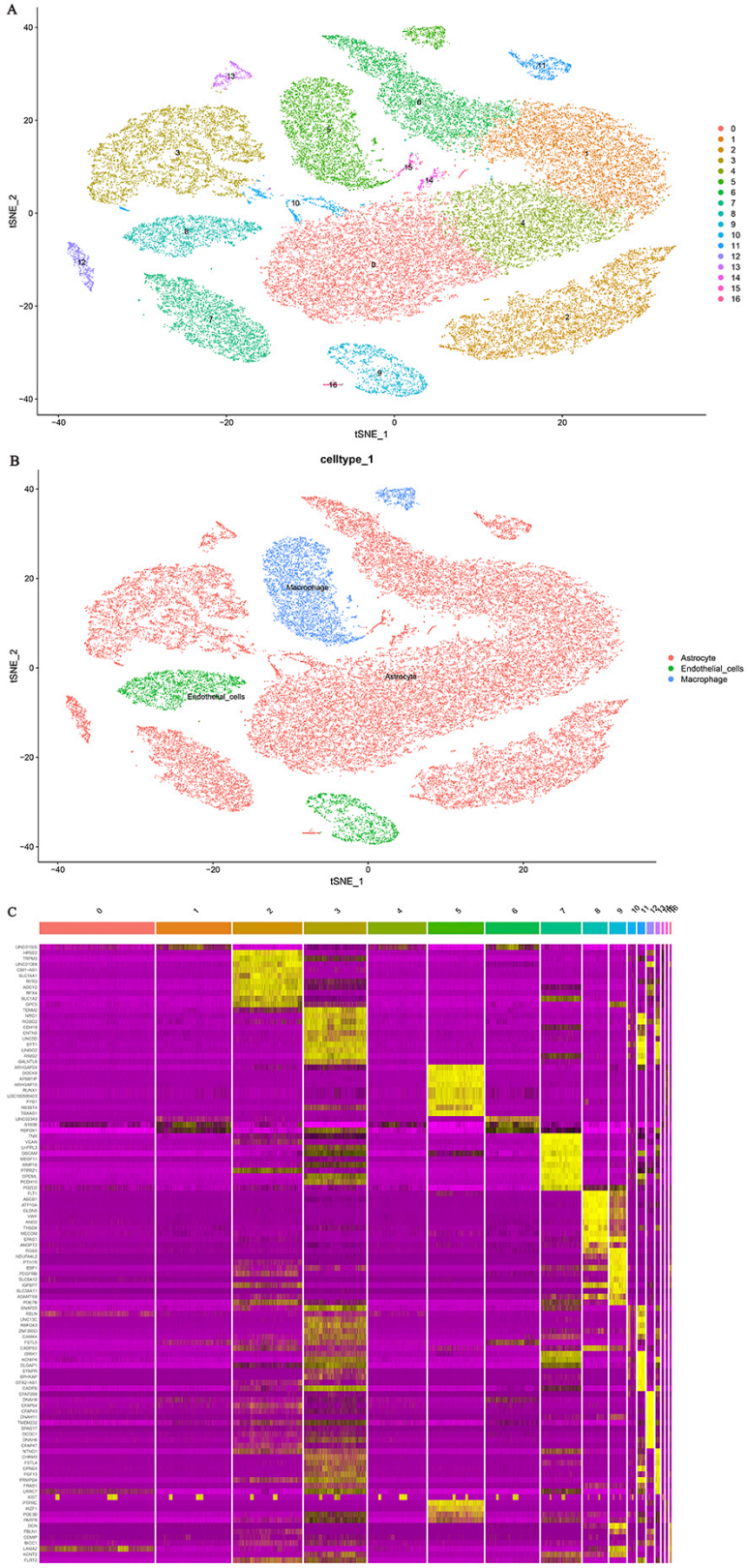

Fig. 1. Single-Cell Transcriptomic Analysis of Parkinson's Disease (PD) and Control Samples. (A) Dimensionality reduction and clustering of the GSE157783 single-cell transcriptomic dataset using the Seurat package in R, resulting in the identification of 17 distinct cell populations. (B) Annotated dimensionality-reduced cluster map of the cell populations, where clusters 0, 1, 2, 3, 4, 6, 7, 10, 11, 12, 13, 14, 15, and 16 correspond to astrocytes, clusters 8 and 9 to endothelial cells, and cluster 5 to macrophages. (C) Heatmap showing the DGE (Differential Gene Expression) across all 17 clusters.

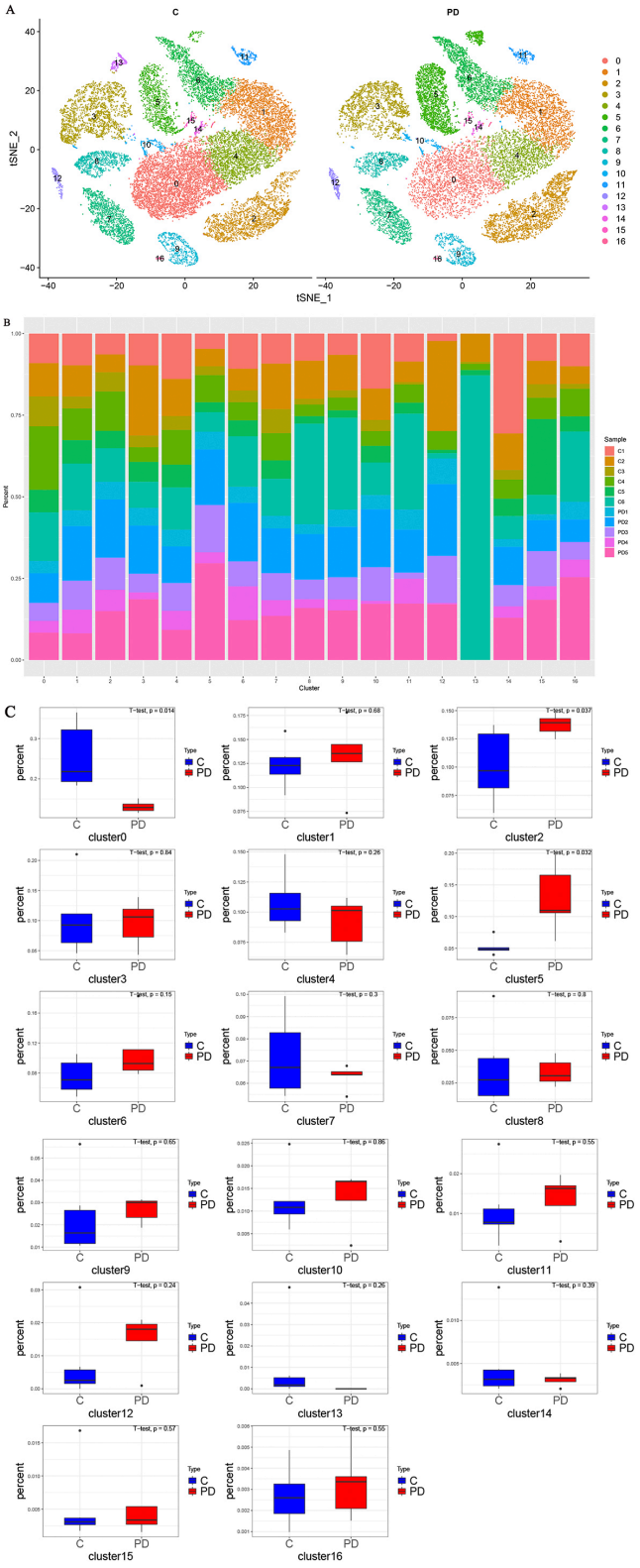

Fig. 2. Comparison of Single-Cell Populations Between PD and Control Groups. (A) Dimensionality-reduced clustering map comparing PD and control groups, highlighting the significant differences in cell populations between the two conditions. (B) Individual-level percentage chart illustrating the proportion of each sample within each cell population, showing the deviation in one normal sample that was excluded from further analysis. (C) Box plots comparing the proportion of each cell population between PD and control groups, with significant differences observed in clusters 0, 2, and 5.

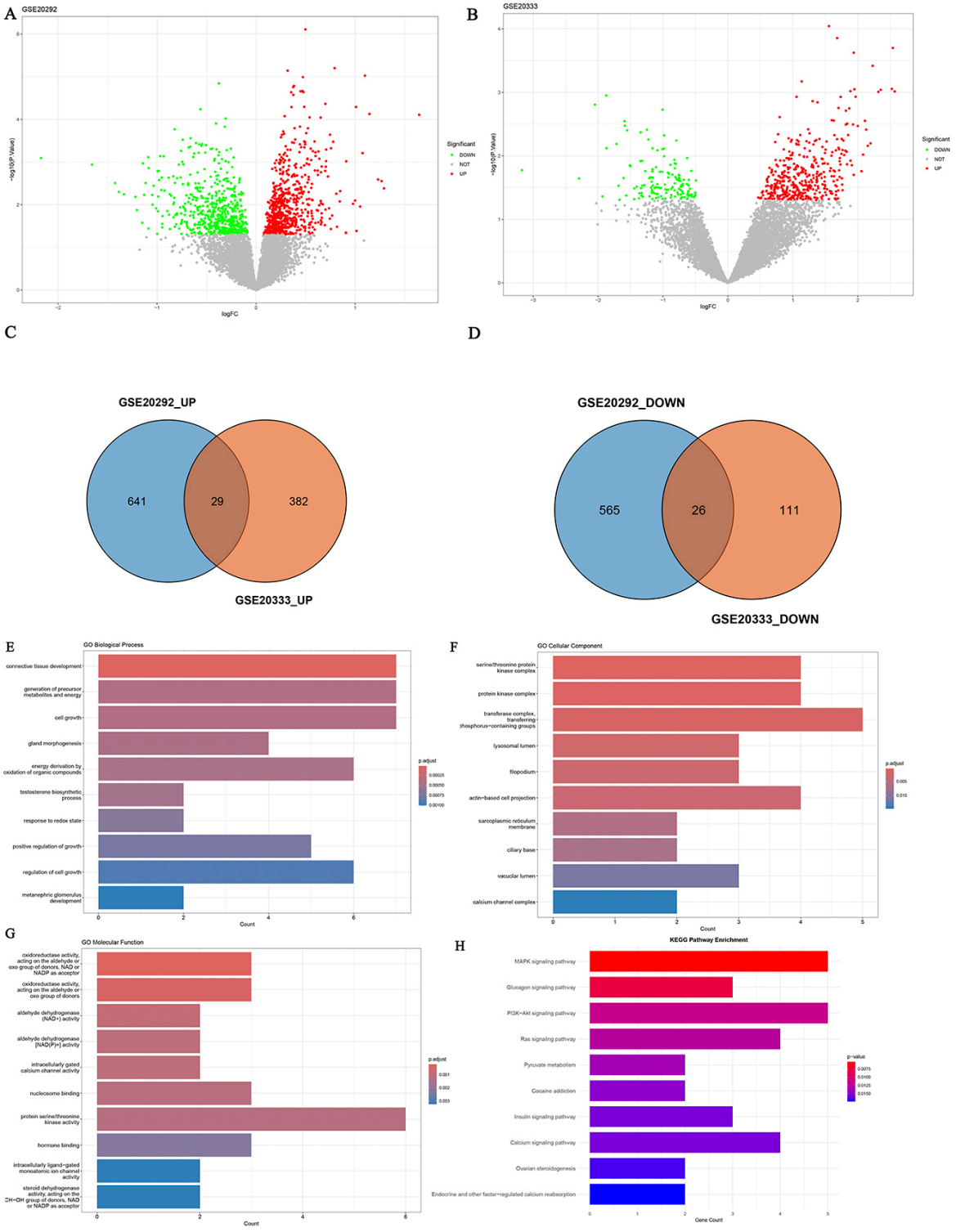

Fig. 3. Differential Gene Expression Analysis of Substantia Nigra Tissue in PD. (A) Volcano plot illustrating the differential gene expression results for the GSE20292 dataset (15 normal controls and 11 PD cases). (B) Volcano plot for the GSE20333 dataset (6 normal controls and 6 PD cases). (C) Venn diagram displaying the 29 upregulated and 26 downregulated genes that are shared between both datasets. (D) Venn diagram of the intersected downregulated genes between the two datasets. (E–H) Gene Ontology (GO) and Kyoto Encyclopedia of Genes and Genomes (KEGG) pathway analysis of the 55 differentially expressed genes, showing the biological processes (GO-BP, E), cellular components (GO-CC, F), molecular functions (GO-MF, G), and enriched pathways (KEGG, H).

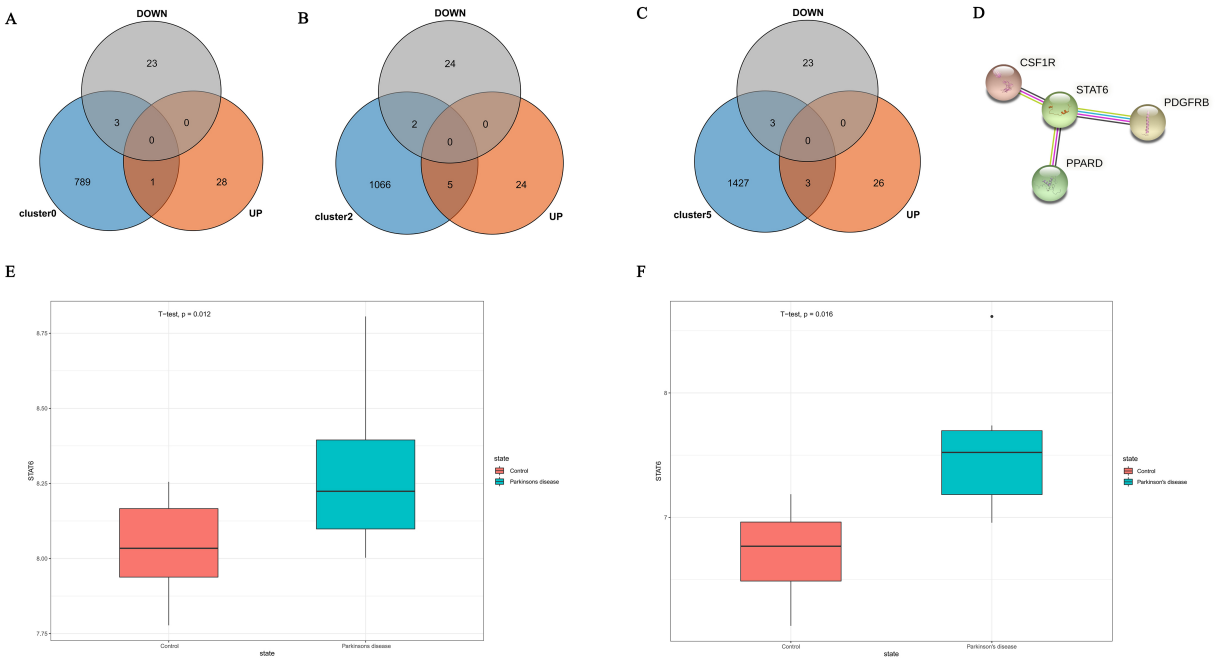

Fig. 4. Identification of Differentially Expressed Genes and the Role of STAT6 in PD Pathogenesis. (A–C) Integration of DEGs from single-cell analysis and tissue-level sequencing. (D) STRING PPI analysis showing interactions between *PDGFRB, CSF1R, STAT6*, and *PPARD*, with *STAT6* at the center, suggesting its key role in PD pathogenesis. (E,F) Box plots comparing the expression of *STAT6* between the PD and control groups in the GSE20292 (E) and GSE20333 (F) datasets. CSF1R, Colony-Stimulating Factor 1 Receptor; PDGFRB, Platelet-Derived Growth Factor Receptor Beta; PPARD, Peroxisome Proliferator-Activated Receptor Delta.

and 26 co-downregulated genes (Fig. 3C Venn diagram of upregulated; Fig. 3D Venn diagram of downregulated). Additionally, Gene Ontology (GO) and Kyoto Encyclopedia of Genes and Genomes (KEGG) pathway analyses were performed on these 55 differentially expressed genes (Fig. 3E for GO-BP; Fig. 3F for GO-CC; Fig. 3G for GO-MF; and Fig. 3H for KEGG). Additionally, correlation analysis revealed an association between STAT6 and genes within the mTOR signaling pathway (**Supplementary Fig. 1A,B**) ($p < 0.05$).

Identification of Differentially Expressed Genes and the Role of STAT6 in PD Pathogenesis

Single-cell analysis demonstrated significant differences in cell populations 0, 2, and 5 between normal individuals and PD patients. Therefore, DEGs from these populations were integrated with those identified through tissue-level sequencing (Fig. 4A–C). Specifically, the downregulated genes included *PRKACB*, *KIF2A*, *SRPK2*, *CHN1*, *ALDH1A1*, *GBE1*, *ZMYM4*, and *UBE2K*, whereas the upregulated genes comprised *CD22*, *RYR1*, *PABPN1*, *PALM*, *PDGFRB*, *SMTN*, *CSF1R*, *STAT6*, and *PPARD*. STRING-based protein-protein interaction analysis showed that *PDGFRB*, *CSF1R*, *STAT6*, and *PPARD* formed a network, with *STAT6* occupying a central position (Fig. 4D). Subsequently, comparison of *STAT6* expression between normal individuals and PD patients in these datasets revealed significantly increased *STAT6* levels in PD patients (Fig. 4E,F, $p < 0.05$), suggesting that *STAT6* plays a pivotal role in PD pathogenesis.

In Vitro Validation of STAT6 Overexpression and Knockdown in PD Model Cells

To further elucidate the role of STAT6 in PD, we conducted a series of *in vitro* cellular experiments. We selected the SH-SY5Y neuroblastoma cell line, commonly employed in neurodegenerative disease research. Initially, STAT6 expression was assessed in an MPP+-induced PD cell model, and cell viability was evaluated after MPP+ induction. The results demonstrated a significant reduction in cell viability in the MPP+ group, confirming successful establishment of the PD model (Fig. 5A) ($p < 0.05$). Subsequent qPCR and Western blot analyses revealed upregulated STAT6 expression in the PD model group compared to controls (Fig. 5B,C) ($p < 0.05$). Based on these observations, 1mM-induced SH-SY5Y cells were used for subsequent experiments. STAT6 knockdown and overexpression were then established in PD model cells, and the efficiency of these manipulations was determined (**Supplementary Fig. 1C,D**) ($p < 0.05$). Hence, siSTAT6-1 was selected for downstream experiments as it demonstrated the highest knockdown efficiency.

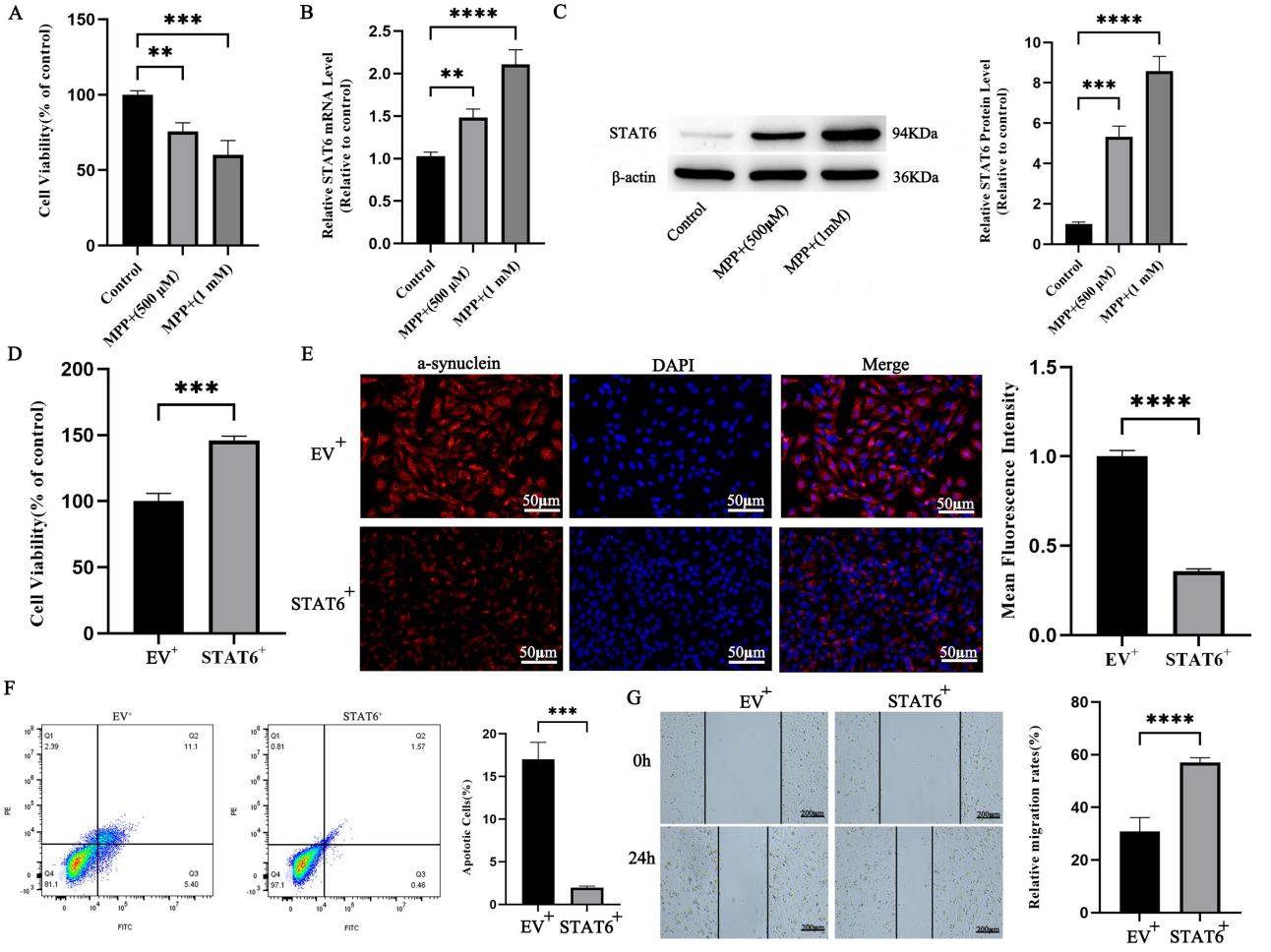

Fig. 5. *In Vitro* Validation of STAT6 Overexpression in PD Model Cells. (A) Cell viability in MPP+-induced PD cells was measured using the MTT assay (N = 3). (B,C) The mRNA and protein levels of STAT6 were assessed using qPCR and Western blot analyses in the 1-methyl-4-phenylpyridinium (MPP+) group compared to the control group (N = 3). (D) The cell viability was determined using the MTT assay in STAT6-overexpressing SH-SY5Y cells compared to the empty vector (EV) group (N = 3). (E) α-Synuclein expression was evaluated using immunofluorescence staining (N = 3). (F) The apoptosis rates were assessed in the STAT6 overexpression group compared to the EV group using Annexin V/PI double staining (N = 3). (G) Cell scratch assay (N = 3). $^{**}p < 0.01$, $^{***}p < 0.001$, $^{****}p < 0.0001$.

Further assessment using the MTT proliferation assay revealed that SH-SY5Y cells overexpressing STAT6 exhibited significantly increased viability compared to the control group (Fig. 5D) ($p < 0.05$). Immunofluorescence staining showed a significant decrease in α-synuclein expression, a crucial pathological marker of PD, in the overexpression group (Fig. 5E) ($p < 0.05$). Apoptosis analysis through Annexin V/PI double staining revealed a significantly lower apoptotic rate in STAT6-overexpressing cells compared to controls (Fig. 5F) ($p < 0.05$). Additionally, a cell scratch assay demonstrated increased migration capability in STAT6-overexpressing cells (Fig. 5G) ($p < 0.05$). Overall, these findings suggest that elevated STAT6 expression in the PD cell model alleviates PD-related pathological phenotypes and exerts a protective role.

We further investigated the impact of STAT6 knockdown on PD model cells. Specifically, SH-SY5Y cells were transfected with siRNA to suppress STAT6 expression. Annexin V/PI double staining indicated a significantly higher apoptosis rate in the STAT6 knockdown group compared to the control groups (Fig. 6A) ($p < 0.05$). MTT assays showed a substantial decrease in cell viability in the STAT6 knockdown group compared to the control group (Fig. 6B) ($p < 0.05$). Additionally, immunofluorescence analysis revealed a significant increase in α-synuclein levels in the STAT6 knockdown group relative to the control groups (Fig. 6C) ($p < 0.05$).

Furthermore, wound healing assays showed that STAT6 knockdown impaired the migration capacity of the cells relative to controls (Fig. 6D) ($p < 0.05$). To examine the impact of STAT6 on oxidative stress, we performed

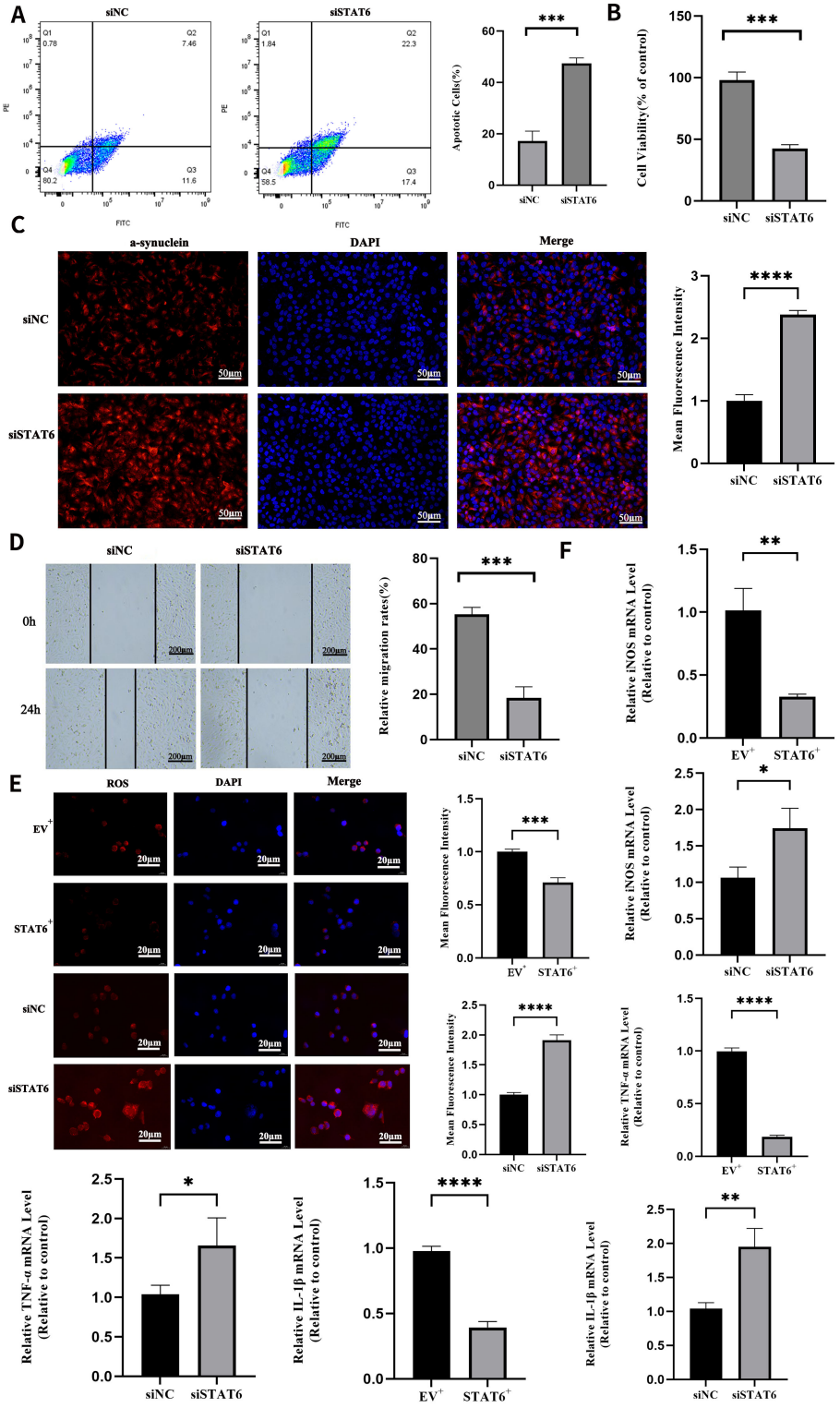

Fig. 6. *In Vitro* Validation of STAT6 Knockdown in PD Model Cells. (A) The apoptosis rates in the STAT6 knockdown group compared to the siNC group were measured through Annexin V/PI double staining (N = 3). (B) The cell viability was determined using the MTT assay (N = 3). (C) α-Synuclein expression was detected through Immunofluorescence staining (N = 3). (D) Wound healing assay (N = 3). (E) Fluorescence-based reactive oxygen species (ROS) detection was performed to measure oxidative stress levels in the PD cell model (N = 3). (F) qRT-PCR analysis of pro-inflammatory cytokine expression levels in PD cell models under conditions of STAT6 overexpression or knockdown (N = 3). Data are presented as mean ± SD, *$p < 0.05$, **$p < 0.01$, ***$p < 0.001$, ****$p < 0.0001$.

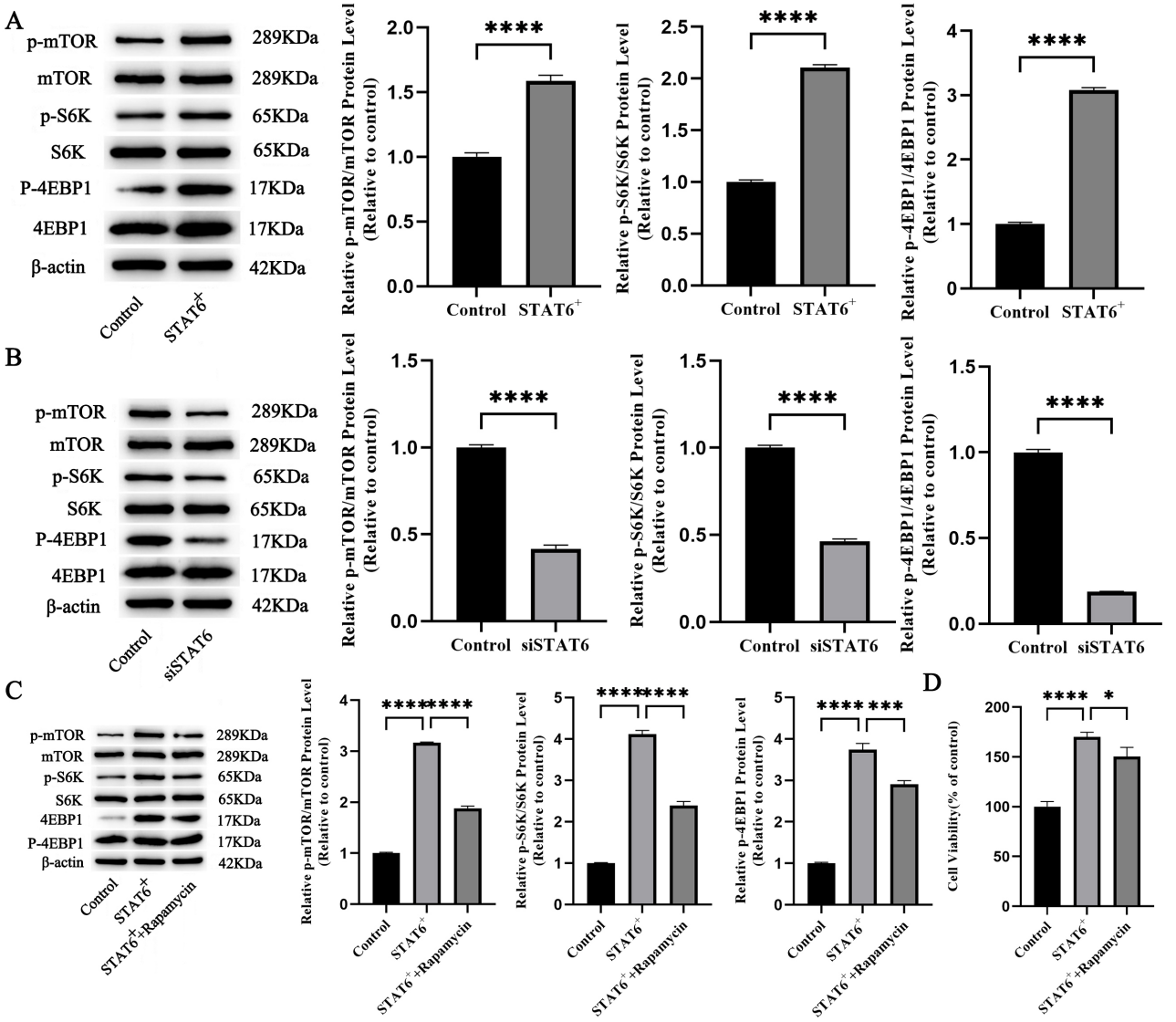

Fig. 7. STAT6 Modulates Mechanistic Target of Rapamycin (mTOR) Signaling in PD Model Cells. (A) Western blot analysis showing the expression of mTOR, S6K (Ribosomal protein S6 kinase), and 4EBP1 (Eukaryotic Translation Initiation Factor 4E-Binding Protein 1) in STAT6-overexpressing SH-SY5Y cells compared to the control group (N = 3). (B) Western blot analysis demonstrating the phosphorylation levels of mTOR, S6K, and 4EBP1 after STAT6 knockdown (N = 3). (C) Western blot analysis indicating the phosphorylation of mTOR, S6K, and 4EBP1 following Rapamycin treatment (N = 3). (D) Cell viability was assessed using MTT assay (N = 3). *$p < 0.05$, ***$p < 0.001$, ****$p < 0.0001$.

fluorescence-based ROS detection. The results showed that STAT6 overexpression significantly reduced intracellular ROS levels, whereas STAT6 inhibition led to a marked increase in ROS levels (Fig. 6E) ($p < 0.05$).

To further investigate the role of STAT6 in neuroinflammation, we quantified the expression of key inflammatory cytokines, including iNOS, TNF-α, and IL-1β, in PD model cells using qRT-PCR. The findings revealed that STAT6 overexpression significantly downregulated the expression of these inflammatory markers, whereas STAT6 inhibition significantly increased their levels (Fig. 6F) ($p < 0.05$). These results indicate that STAT6 plays a crucial role in modulating neuroinflammatory responses in PD. Collectively, these findings suggest that STAT6 knockdown enhances neuronal apoptosis, oxidative stress, and inflammation in PD model cells.

STAT6 Modulates mTOR Signaling in PD Model Cells

In SH-SY5Y cells, STAT6 overexpression was successfully achieved through transfection with an expression vector harboring the STAT6 gene (**Supplementary Fig. 1D**). Western blot analysis revealed that the phosphorylation levels of mTOR, S6K (Ribosomal protein S6 ki-

nase), and 4EBP1 (Eukaryotic Translation Initiation Factor 4E-Binding Protein 1) were significantly elevated in the STAT6-overexpressing group compared to the control group (Fig. 7A) ($p < 0.05$), indicating enhanced activation of the mTOR signaling pathway. These findings suggest that STAT6 overexpression may positively modulate the mTOR signaling cascade.

To further elucidate the role of STAT6 in mTOR signaling, we employed siRNA-mediated knockdown of STAT6 expressions. The results demonstrated a significant reduction in the phosphorylation levels of mTOR, S6K, and 4EBP1 following STAT6 knockdown (Fig. 7B) ($p < 0.05$), which is consistent with the effects observed in STAT6 overexpression, thereby underscoring the crucial role of STAT6 in regulating the mTOR pathway. Given the potential interplay between STAT6 and mTOR signaling, we investigated the impact of the mTOR inhibitor Rapamycin on PD model cells. Western blot analysis demonstrated that Rapamycin treatment substantially diminished the phosphorylation levels of mTOR, S6K, and 4EBP1 (Fig. 7C) ($p < 0.05$). Additionally, MTT assays showed that Rapamycin exposure significantly reduced cell viability in PD model cells (Fig. 7D) ($p < 0.05$). Collectively, these results indicate that the increased phosphorylation of mTOR mediates, at least in part, the effects of STAT6 overexpression in the PD cell model.

Discussion

In this study, we identified STAT6 as a key mediator in PD progression, highlighting its potential role in regulating neuroinflammation and cellular dysfunction. Our findings align with the growing body of evidence implicating inflammatory pathways in the pathophysiology of PD. We observed that STAT6 overexpression protects critical pathological features of PD, including neuronal apoptosis, α-synuclein accumulation, and impaired cell migration. In contrast, STAT6 knockdown worsens these pathological changes, suggesting that STAT6 plays a protective role against neuronal damage in PD. Notably, these effects were linked to the activation of the mTOR signaling pathway, a crucial regulator of cell survival, protein synthesis, and autophagy.

In ischemic stroke, STAT6 deficiency has been reported to impair the phagocytosis of apoptotic neurons, aggravate neuroinflammation, expand cerebral infarction volume, and cause persistent neurological dysfunction [16]. Using single-cell transcriptomic analysis, we identified significant differences in cell populations between normal individuals and PD patients, particularly within astrocytes and macrophages, both of which are involved in neuroinflammation. STAT6 was found to be a key upregulated gene across both single-cell and tissue-level datasets, supporting its role in modulating the inflammatory microenvironment in the PD brain [17,18]. Previous research has emphasized the significance of pro-inflammatory cytokines driving neurodegeneration [19,20], and through its regulation of immune responses, STAT6 may influence this activation, potentially contributing to PD progression.

MPP+-treated SH-SY5Y cells are widely used as a standard *in vitro* cellular model for PD [21]. Furthermore, our *in vitro* experiments using the SH-SY5Y PD cell model showed that STAT6 overexpression led to decreased apoptosis and enhanced cell viability, both of which are characteristic features of neurodegeneration in PD [22,23]. Conversely, STAT6 knockdown increased apoptosis, reduced cell survival, and impaired cell migration, suggesting its potential as a therapeutic target. These findings are consistent with studies revealing that modulating STAT6 may protect against neuroinflammation and neuronal death in neuroinflammatory diseases [16,18,24].

The mTOR signaling pathway regulates diverse cellular processes, including autophagy, apoptosis, and metabolism [25–27]. The connection between STAT6 and the mTOR pathway offers additional insights into the molecular mechanisms underlying PD [28]. A previous study has reported that STAT6 can negatively regulate mTOR, potentially through hypoxia-induced stimulation by HIF-1α (Hypoxia-Inducible Factor 1-αlpha subunit), a key regulator of mTOR [29]. Our results show that STAT6 overexpression activates the mTOR signaling cascade, which is critical for regulating cellular metabolism, growth, and survival. Under the hypoxic conditions in glioma, STAT6 inhibits mTOR by directly binding to Rheb to suppress tumor progression. Conversely, in the neuroinflammatory environment of PD, STAT6 activates mTOR to promote neuronal survival and reduce the toxicity of α-synuclein. Consistently, inhibition of mTOR signaling with Rapamycin increased apoptosis and reduced cell viability in PD model cells, suggesting that mTOR mediates the protective effects of STAT6 in PD. Emerging evidence suggests that restoring disrupted mTOR signaling in PD models can inhibit neuronal cell death [14,30], highlighting the therapeutic potential of targeting the STAT6-mTOR axis to modulate neuroinflammation and protect against neuronal damage in PD.

It is crucial to acknowledge the limitations of this study. First, although SH-SY5Y cells are commonly utilized as a cellular model for PD, they may not completely mirror the intricate pathophysiology of PD within the human brain. Second, while our results demonstrate the effects of STAT6 modulation *in vitro*, additional *in vivo* investigations are necessary to validate these findings and to evaluate the therapeutic potential of STAT6-targeted approaches in animal models of PD. Additionally, the exact mechanisms by which STAT6 affects mTOR signaling and its subsequent downstream outcomes remain incompletely understood. Future research should focus on elucidating the molecular pathways that directly link STAT6 to mTOR and their impact on PD pathology.

Conclusion

In conclusion, our study emphasizes STAT6 as a key modulator in PD pathology. Knockdown of STAT6 exacerbates neuroinflammation and neurodegeneration, whereas its overexpression offers neuroprotective effects. Our findings further suggest that the STAT6-mTOR axis could be a promising therapeutic target for alleviating PD progression. However, further research is required to fully understand the complex interactions between STAT6, mTOR, and other signaling pathways involved in PD.

Availability of Data and Materials

The data used to support the findings of this study are included within the article.

Author Contributions

XQM and YNT designed the research study; XMS and YL performed the research; LC, HBY and QL collected and analyzed the data. XQM and YNT have been involved in drafting the manuscript and all authors have been involved in revising it critically for important intellectual content. All authors gave final approval of the version to be published. All authors have participated sufficiently in the work to take public responsibility for appropriate portions of the content and agreed to be accountable for all aspects of the work in ensuring that questions related to its accuracy or integrity.

Ethics Approval and Consent to Participate

Not applicable.

Acknowledgment

Not applicable.

Funding

This study was funded by Qiqihar Science and Technology Tackling Project (LSFGG-2024024).

Conflict of Interest

The authors declare no conflict of interest.

Supplementary Material

Supplementary material associated with this article can be found, in the online version, at https://doi.org/10.24976/Discov.Med.202537202.229.

References

[1] Simon DK, Tanner CM, Brundin P. Parkinson Disease Epidemiology, Pathology, Genetics, and Pathophysiology. Clinics in Geriatric Medicine. 2020; 36: 1–12. https://doi.org/10.1016/j.cger.2019.08.002.

[2] Xiong LL, Du RL, Niu RZ, Xue LL, Chen L, Huangfu LR, *et al*. Single-cell RNA sequencing reveals peripheral immunological features in Parkinson's Disease. NPJ Parkinson's Disease. 2024; 10: 185. https://doi.org/10.1038/s41531-024-00790-3.

[3] Karpathiou G, Papoudou-Bai A, Ferrand E, Dumollard JM, Peoc'h M. STAT6: A review of a signaling pathway implicated in various diseases with a special emphasis in its usefulness in pathology. Pathology, Research and Practice. 2021; 223: 153477. https://doi.org/10.1016/j.prp.2021.153477.

[4] Wei L, Vahedi G, Sun HW, Watford WT, Takatori H, Ramos HL, *et al*. Discrete roles of STAT4 and STAT6 transcription factors in tuning epigenetic modifications and transcription during T helper cell differentiation. Immunity. 2010; 32: 840–851. https://doi.org/10.1016/j.immuni.2010.06.003.

[5] Huang W, Hong Y, He W, Jiang L, Deng W, Peng B, *et al*. Cavin-1 promotes M2 macrophages/microglia polarization via SOCS3. Inflammation Research: Official Journal of the European Histamine Research Society ... [et Al.]. 2022; 71: 397–407. https://doi.org/10.1007/s00011-022-01550-w.

[6] Soliman E, Leonard J, Basso EKG, Gershenson I, Ju J, Mills J, *et al*. Efferocytosis is restricted by axon guidance molecule EphA4 via ERK/Stat6/MERTK signaling following brain injury. Journal of Neuroinflammation. 2023; 20: 256. https://doi.org/10.1186/s12974-023-02940-5.

[7] Nishimura Y, Nitto T, Inoue T, Node K. STAT6 mediates apoptosis of human coronary arterial endothelial cells by interleukin-13. Hypertension Research: Official Journal of the Japanese Society of Hypertension. 2008; 31: 535–541. https://doi.org/10.1291/hypres.31.535.

[8] Chao H, Zheng L, Hsu P, He J, Wu R, Xu S, *et al*. IL-13RA2 downregulation in fibroblasts promotes keloid fibrosis via JAK/STAT6 activation. JCI Insight. 2023; 8: e157091. https://doi.org/10.1172/jci.insight.157091.

[9] Lv T, Zhang Z, Yu H, Ren S, Wang J, Li S, *et al*. Tamoxifen Exerts Anticancer Effects on Pituitary Adenoma Progression via Inducing Cell Apoptosis and Inhibiting Cell Migration. International Journal of Molecular Sciences. 2022; 23: 2664. https://doi.org/10.3390/ijms23052664.

[10] Liu GY, Sabatini DM. mTOR at the nexus of nutrition, growth, ageing and disease. Nature Reviews. Molecular Cell Biology. 2020; 21: 183–203. https://doi.org/10.1038/s41580-019-0199-y.

[11] Saxton RA, Sabatini DM. mTOR Signaling in Growth, Metabolism, and Disease. Cell. 2017; 168: 960–976. https://doi.org/10.1016/j.cell.2017.02.004.

[12] Swiech L, Perycz M, Malik A, Jaworski J. Role of mTOR in physiology and pathology of the nervous system. Biochimica et Biophysica Acta. 2008; 1784: 116–132. https://doi.org/10.1016/j.bbapap.2007.08.015.

[13] Zhou Q, Liu C, Liu W, Zhang H, Zhang R, Liu J, *et al*. Rotenone induction of hydrogen peroxide inhibits mTOR-mediated S6K1 and 4E-BP1/eIF4E pathways, leading to neuronal apoptosis. Toxicological Sciences: An Official Journal of the Society of Toxicology. 2015; 143: 81–96. https://doi.org/10.1093/toxsci/kfu211.

[14] Lan AP, Chen J, Zhao Y, Chai Z, Hu Y. mTOR Signaling in Parkinson's Disease. Neuromolecular Medicine. 2017; 19: 1–10. https://doi.org/10.1007/s12017-016-8417-7.

[15] Lee H, Ju IG, Kim JH, Choi Y, Lee S, Park HJ, *et al*. Artemisiae Iwayomogii Herba Protects Dopaminergic Neurons Against 1-Methyl-4-phenylpyridinium/1-methyl-4-phenyl-1,2,3,6-tetrahydropyridine Neurotoxicity in Models of Parkinson's Disease. Nutrients. 2025; 17: 1672. https://doi.org/10.3390/nu17101672.

[16] Cai W, Dai X, Chen J, Zhao J, Xu M, Zhang L, *et al*. STAT6/Arg1 promotes microglia/macrophage efferocytosis and inflammation resolution in stroke mice. JCI Insight. 2019; 4: e131355. https://doi.org/10.1172/jci.insight.131355.

[17] Hsu CH, Pan YJ, Zheng YT, Lo RY, Yang FY. Ultrasound reduces inflammation by modulating M1/M2 polarization of microglia through STAT1/STAT6/PPARγ signaling pathways. CNS Neuroscience & Therapeutics. 2023; 29: 4113–4123. https://doi.org/10.1111/cns.14333.

[18] Olde Heuvel F, Holl S, Chandrasekar A, Li Z, Wang Y, Rehman R, *et al*. STAT6 mediates the effect of ethanol on neuroinflammatory response in TBI. Brain, Behavior, and Immunity. 2019; 81: 228–246. https://doi.org/10.1016/j.bbi.2019.06.019.

[19] Marogianni C, Sokratous M, Dardiotis E, Hadjigeorgiou GM, Bogdanos D, Xiromerisiou G. Neurodegeneration and Inflammation-An Interesting Interplay in Parkinson's Disease. International Journal of Molecular Sciences. 2020; 21: 8421. https://doi.org/10.3390/ijms21228421.

[20] Isik S, Yeman Kiyak B, Akbayir R, Seyhali R, Arpaci T. Microglia Mediated Neuroinflammation in Parkinson's Disease. Cells. 2023; 12: 1012. https://doi.org/10.3390/cells12071012.

[21] Song Q, Peng S, Zhu X. Baicalein protects against MPP+/MPTP-induced neurotoxicity by ameliorating oxidative stress in SH-SY5Y cells and mouse model of Parkinson's disease. Neurotoxicology. 2021; 87: 188–194. https://doi.org/10.1016/j.neuro.2021.10.003.

[22] Li J, Chen L, Qin Q, Wang D, Zhao J, Gao H, *et al*. Upregulated hexokinase 2 expression induces the apoptosis of dopaminergic neurons by promoting lactate production in Parkinson's disease. Neurobiology of Disease. 2022; 163: 105605. https://doi.org/10.1016/j.nbd.2021.105605.

[23] Lei T, Fu G, Xue X, Yang H. Tianma Gouteng Decoction improve neuronal synaptic plasticity and oligodendrocyte apoptosis in Parkinson's disease mice. Phytomedicine: International Journal of Phytotherapy and Phytopharmacology. 2025; 140: 156553. https://doi.org/10.1016/j.phymed.2025.156553.

[24] Liu X, Wang J, Jin J, Hu Q, Zhao T, Wang J, *et al*. S100A9 deletion in microglia/macrophages ameliorates brain injury through the STAT6/PPARγ pathway in ischemic stroke. CNS Neuroscience & Therapeutics. 2024; 30: e14881. https://doi.org/10.1111/cns.14881.

[25] Frake RA, Ricketts T, Menzies FM, Rubinsztein DC. Autophagy and neurodegeneration. The Journal of Clinical Investigation. 2015; 125: 65–74. https://doi.org/10.1172/JCI73944.

[26] Li Y, Zhou Y, Liu D, Wang Z, Qiu J, Zhang J, *et al*. Glutathione Peroxidase 3 induced mitochondria-mediated apoptosis via AMPK /ERK1/2 pathway and resisted autophagy-related ferroptosis via AMPK/mTOR pathway in hyperplastic prostate. Journal of Translational Medicine. 2023; 21: 575. https://doi.org/10.1186/s12967-023-04432-9.

[27] Szwed A, Kim E, Jacinto E. Regulation and metabolic functions of mTORC1 and mTORC2. Physiological Reviews. 2021; 101: 1371–1426. https://doi.org/10.1152/physrev.00026.2020.

[28] Deltas C, Felekkis K. Is suppression of cyst growth in PKD enough to preserve renal function?: STAT6 inhibition is a novel promising target. JAK-STAT. 2012; 1: 216–218. https://doi.org/10.4161/jkst.21634.

[29] Park SJ, Kim H, Kim SH, Joe EH, Jou I. Epigenetic downregulation of STAT6 increases HIF-1α expression via mTOR/S6K/S6, leading to enhanced hypoxic viability of glioma cells. Acta Neuropathologica Communications. 2019; 7: 149. https://doi.org/10.1186/s40478-019-0798-z.

[30] Yu L, Hu X, Xu R, Zhao Y, Xiong L, Ai J, *et al*. Piperine promotes PI3K/AKT/mTOR-mediated gut-brain autophagy to degrade α-Synuclein in Parkinson's disease rats. Journal of Ethnopharmacology. 2024; 322: 117628. https://doi.org/10.1016/j.jep.2023.117628.